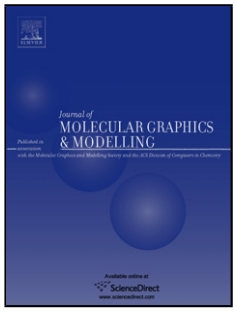

Title: Understanding the molecular mechanism and regioselectivity in the synthesis of celecoxib via a domino reaction: A DFT study

Author: Saeed Reza Emamian

PII: S1093-3263(15)00084-4
DOI: http://dx.doi.org/doi:10.1016/j.jmgm.2015.05.006
Reference: JMG 6546

To appear in: *Journal of Molecular Graphics and Modelling*

Received date: 4-11-2014
Revised date: 4-4-2015
Accepted date: 13-5-2015

Please cite this article as: S.R. Emamian, Understanding the molecular mechanism and regioselectivity in the synthesis of celecoxib via a domino reaction: A DFT study, *Journal of Molecular Graphics and Modelling* (2015), http://dx.doi.org/10.1016/j.jmgm.2015.05.006

Understanding the molecular mechanism and regioselectivity in the synthesis of celecoxib via a domino reaction: A DFT study

Saeed Reza Emamian*

Chemistry Department, Shahrood Branch, Islamic Azad University, Shahrood, Iran

Abstract

The molecular mechanism and energetic of the domino reaction involved in the synthesis of celecoxib, a well-known anti-inflammatory drug, were theoretically studied at the DFT-B3LYP/6-31G* level. The first reaction in this domino process, which is also the rate-determining step, is a complete regioselective [3+2] cycloaddition (32CA) reaction associated with the nucleophilic attack of C5 carbon atom of enamine **7** on the C3 carbon atom of nitrile imine **6**, leading to cycloadduct **8**. The second reaction is a rapid acid/base catalysed stepwise elimination reaction of the morpholine **9** from cycloadduct **8** affording celecoxibe **3**. The results also show that neither molecular mechanism of reaction nor activation barriers are considerably affected by the inclusion of solvent. The calculated relative Gibbs free energies as well as local reactivity indices obtained using the calculated Parr functions explain the complete regioselective fashion provided by the 32CA reaction under consideration in excellent agreement with the experimental findings.

Keywords: Celecoxib; Nitrile imine; Regioselectivity; DFT reactivity indexes; Parr functions

* Corresponding author. Tel.: +989121735085; Fax: +98 23 32390537.

E-mail address: s_emamian@iau-shahrood.ac.ir & saeedreza_em@yahoo.com

1. Introduction

Nitrogen-containing heterocycles are biologically interesting compounds [1]. Pyrazoles are an important class of nitrogen-containing heterocycles comprising two adjacent nitrogen atoms in a five-membered ring which are extensively used in the pharmaceutical industry [2]. The compounds bearing pyrazole nucleus are well known to exhibit versatile range of biological activities such as antiviral, antiparasitic, antitumor, antibacterial and antifungal, insecticidal, and anti-tubercular agents [3,4]. Moreover, the applicability of these heterocycles has also been known in the agrochemical industry and, recently, in the field of photoprotectors, energetic materials and ultraviolet stabilizers [5]. Owing to such extensive applications and in particular biological notability, pyrazoles have received remarkable attention in recent years.

Celecoxib **3**, a well-known anti-inflammatory drug [6], is a 1,3,5-trisubstituted pyrazole derivative providing COX-2 inhibitor activity. Celecoxib **3** can be obtained using a general strategy in which 4-sulfamidophenylhydrazine **1** reacts with diketone **2** producing a regioisomeric mix of both pyrazoles **3** and **4** (see Scheme 1). In this approach, in order to obtain celecoxib **3**, a recrystallization step should be included [7].

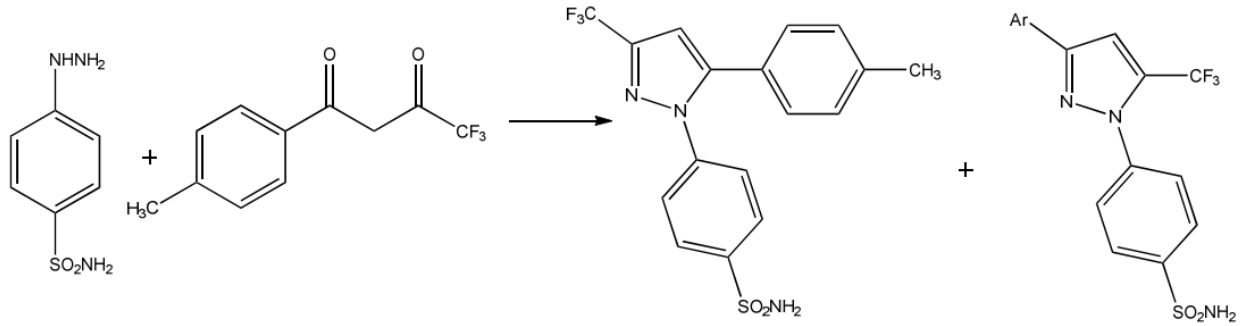

1 **2** Celecoxib **3** **4**

Scheme 1

Oh has recently introduced a simple, practical, and straightforward protocol for synthesis of celecoxib **3** [7]. In this manner, the preparation of celecoxib **3** was accomplished via a complete regioselective [3+2] cycloaddition (32CA) reaction between nitrile imine **6**, generated *in situ* from hydrazonoyl benzenesulfonate **5**, and enamine **7** in good yield of 72% (see Scheme 2).

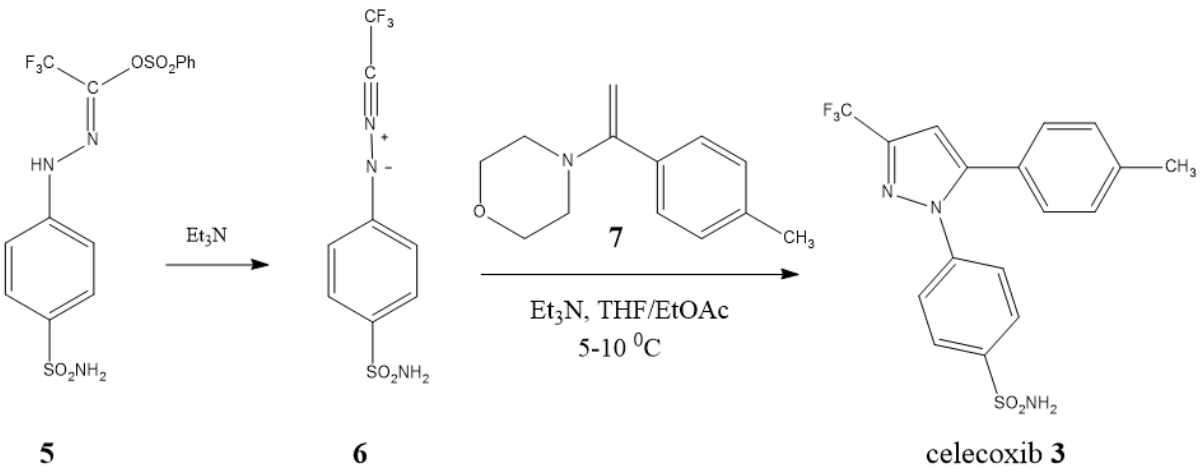

5 6

Scheme 2

Herein, the molecular mechanism and energetic study of reaction between nitrile imine **6** and enamine **7** yielding celecoxib **3** are performed at the DFT-B3LYP/6-31G* level (see Scheme 3). This reaction is a domino process initialised by a 32CA reaction between nitrile imine **6** and enamine **7** affording the cycloadduct (CA) **8** followed by a rapid acid/base catalysed morpholine elimination yielding celecoxib **3**.

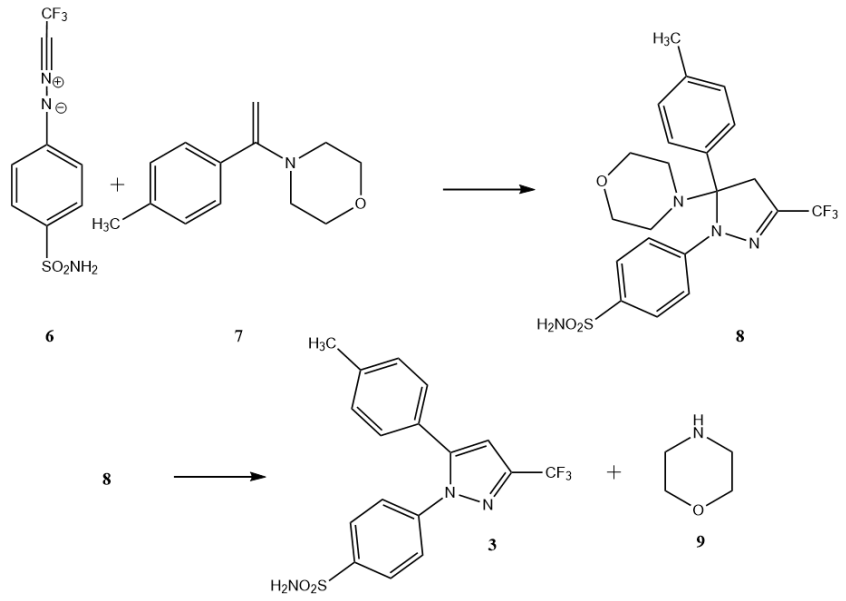

Scheme 3. Plausible mechanism for the domino reaction between nitrile imine **6** and enamine**7** yielding celecoxib **3**.

2. Computational details

Previous theoretical studies devoted to the 32CA reactions have confirmed that using DFT/B3LYP method together with the standard 6-31G* basis set is appropriate to obtain reliable geometries and energies [8,9]. Consequently, in the present work, geometries of all stationary points in the gas phase as well as in the presence of solvent were fully optimised using density functional theory with the B3LYP [10] exchange correlation functional and 6-31G* basis set. The optimisations were carried out by means of the Berny analytical gradient optimisation method using GEDIIS [11]. The IRC paths [12] were traced in order to check the energy profiles connecting each TS to the two associated minima of the proposed mechanism using the Hessian-based Predictor-Corrector (HPC) integrator algorithm [13,14]. Solvent effects of tetrahydrofuran (THF), the solvent considered experimentally, were taken into account using the polarisable continuum model (PCM) as developed by Tomasi's group [15] in the framework of the self-consistent reaction field (SCRF) [16-18]. To confirm the nature of stationary points located on the potential energy surface (PES) and evaluate the Gibbs free energies, frequency calculations were carried out at 298.15 K and 1.0 atm. For minimum state structures and for the TSs, only real frequency values and only a single imaginary frequency value were accepted, respectively. The normal modes corresponding to the imaginary frequencies in the transition state structures are related to the vibrations of the new developing bonds. The electronic structures of stationary points were analysed by the natural bond orbital (NBO) method [19]. The global electrophilicity index, introduced by Parr *et al.* [20], is given by the following expression, $\omega = (\mu^2/2\ \eta)$, in terms of the electronic chemical potential, μ, and the chemical hardness, η. Koopman's theorem [21]

allows to evaluate μ as $(\varepsilon_H + \varepsilon_L)/2$ and η as $(\varepsilon_L - \varepsilon_H)$ where ε_H and ε_L indicate the energy of highest occupied molecular orbital (HOMO) and lowest unoccupied molecular orbital (LUMO), respectively [8]. Recently, Domingo *et al*. [22] have introduced an empirical (relative) nucleophilicity index as $N = \varepsilon_{H(Nu)} - \varepsilon_{H(TCE)}$. In this index, the difference between HOMO energies of nucleophile (Nu) and tetracyanoethylene (TCE), as reference, is considered. This is worth to note that this definition leads to positive value for nucleophilicity index because TCE presents lowest HOMO energy in a large series of molecule investigated in the context of polar cycloadditions. The electrophilic, P_k^+, and nucleophilic, P_k^-, Parr functions were obtained using methodology which has very recently been proposed by Domingo *et al*. [23]. With these values at hand, local electrophilicity index, ω_k, and local nucleophilicity index, N_k, can easily be obtained as $\omega_k = \omega P_k^+$ and $N_k = N P_k^-$ [23]. All calculations were carried out using Gaussian 09 computational program package [24].

3. Results and discussion

The present theoretical study is divided into two parts: (i) first, a complete characterisation of the molecular mechanism and energetic of the domino reaction between nitrile imine **6** and enamine **7** yielding celecoxib **3** is presented; (ii) then, a DFT analysis based on the global and local reactivity indexes for reactants will be carried out in order to explain reactivity and regioselectivity of the 32CA reaction between nitrile imine **6** and enamine **7**.

*(i) Study of the molecular mechanism and energetic of the domino reaction between nitrile imine **6** and enamine **7**.*

This domino process begins by a 32CA reaction between nitrile imine **6** and enamine **7** affording CA **8** which in turn undergoes an acid/base catalysed stepwise elimination of morpholine **9** furnishing celecoxib **3**. Due to the asymmetric nature of both reactants, two different regioisomeric pathways associated with the N1-C5 and N1-C4 forming bonds are feasible. The proposed mechanism for this domino reaction including atoms numbering is presented in scheme 4. Based on the analysis of the stationary points, these 32CA reactions take place through a one-step mechanism. Consequently, two regioisomeric TSs, **TS1** and **TS2**, and two CAs **8** and **10** were located and characterised. The Gibb free energies including its relative values in the gas phase as well as in THF are given in Table 1. As shown in this table, while the absolute values of Gibbs free energies are noticeably affected by solvent, the relative values except for the steps corresponded to the formation of protonated CA **11** and celecoxib **3** are not significantly changed by the inclusion of solvent. The activation Gibbs free energies in the presence of THF associated with the two N1-C5 and N1-C4 regioisomeric channels are 14.8 (**TS1**) and 27.7 (**TS2**) kcal/mol, respectively. Moreover, 32CA reactions are strongly exergonic; -28.5 (**8**) and -30.8 (**10**) kcal/mol. Two appealing conclusions can be obtained considering these results: i) **TS1** is located 12.9 kcal/mol below the **TS2** indicating that the 32CA reaction between nitrile imine **6** and enamine **7** takes place completely regioselective via N1-C4 channel passing through **TS1**; and ii) the high exergonic character associated with either channel allows these 32CA reactions to be irreversible.

The second reaction of this domino process is the elimination of morpholine **9** from CA **8** to yield celecoxib **3**. This elimination reaction has an acid/base catalysed stepwise mechanism; the first step is the extrusion of morpholine from **8** through the C_a-N_b breaking bond (C_a and N_b are denoted in scheme 4). This process is acid catalysed in order to generate a good leaving ammonium group. Protonation of the N_b nitrogen atom of **8** does not provide an appreciable barrier; the proton transfer process from oxonium cation to **8** leading to the formation of protonated CA **11** together with water being exergonic by 19.3 kcal/mol. The extrusion of morpholine **9** from the protonated CA **11** via **TS4** has a very low activation Gibbs free energy of 1.2 kcal/mol. Moreover, the formation of cationic intermediate **12** together with morpholine **9** is exergonic by 23.7 kcal/mol. The last step of this stepwise elimination is a proton extraction from the

cationic intermediate **12** yielding celecoxib **3**. This step can be promoted by morpholine **9** generated in the previous step. In the gas phase, the TS associated with this proton abstraction via **TS4** presents a very low activation Gibbs free energy of 0.2 kcal/mol. It is worth to note that any attempt to locate **TS4** in THF was unsuccessful.

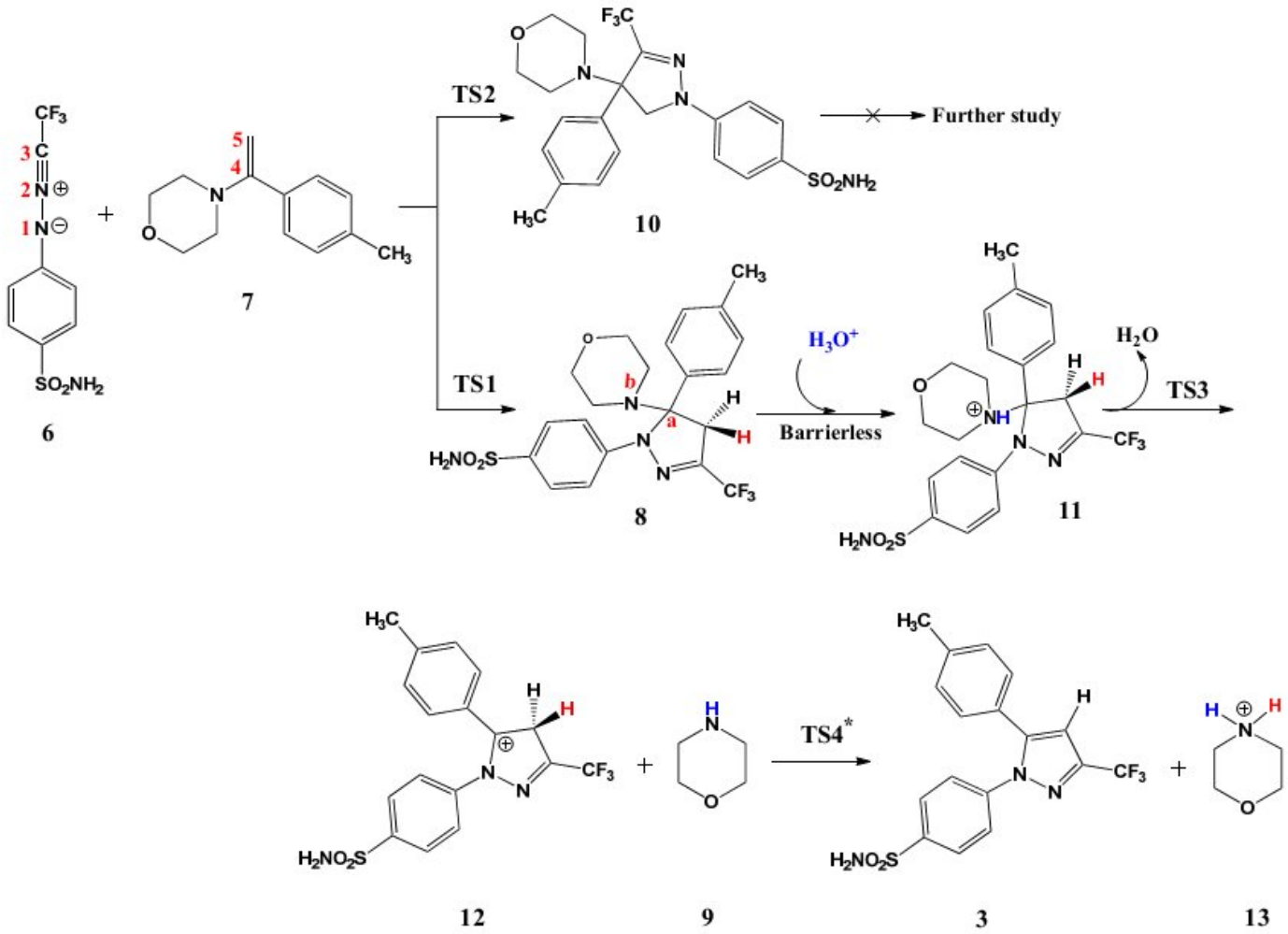

Scheme 4. Proposed mechanism including atoms numbering for the domino reaction between nitrile imine **6** and enamine **7** yielding more favorable regioisomeric celecoxib **3**. (* any attempt to locate TS4 failed in the presence of THF).

A schematic representation of the Gibbs free energy profile for the studied domino reaction, presented in scheme 4, is sketched in Fig. 1. As can be seen, the first 32CA reaction constitutes the rate-determining step of this domino process. After formation of CA **8**, the stepwise elimination of morpholine **9** yielding celecoxib **3** has not appreciable barrier.

The optimised geometries of the TSs involved in the 32CA reaction between nitrile imine **6** and enamine **7**, **TS1** and **TS2**, and those involved in the morpholine elimination reaction, **TS3** and **TS4**, are given in Fig. 2. The lengths of the C-N and C-C forming bonds at the two regioisomeric TSs are 3.73 and 2.40 Å at **TS1** and 2.18 and 2.54 Å at **TS2**, respectively. On the other hand, the Wiberg bond orders [25] of the two C-C and C-N forming bonds are 0.20 and 0.03 at **TS1** and, 0.23 and 0.33 at **TS2**, respectively. The extent of the synchronicity associated with the either of regioisomeric pathways can simply be measured as the difference between the Wiberg bond orders, ΔBO, of the two forming bonds at the corresponding TS [26]. The absolute values of ΔBO for **TS1** and **TS2** are 0.17 and 0.10, respectively, indicating that the most favorable **TS1** presents a lower degree of synchronicity than **TS2**. On the other hand, analysis of the atomic motion at the unique imaginary frequency of **TS1** obviously shows that this motion is mainly associated with the C3 and C5 atoms along C3-C5 bond-forming path, the movement of the N1 and C4 atoms being negligible. In spite of high asynchronicity found in **TS1**, any attempt to locate a stable intermediate associated with the two-center C3-C5 attack along N1-C4 regioisomeric pathway failed indicating that 32CA reaction between nitrile imine **6** and enamine **7** in the more favorable regioisomeric **TS1** takes place via a *one-step two-stage* mechanism [27], i.e. while the C3-C5 bond formation takes place along the nucleophilic attack of the C5 carbon atom of enamine **7** on the C3 carbon atom of nitrile imine **6** in the first stage of the reaction, the N1-C4 bond formation is carried out in the second stage once the first C3-C5 bond is practically formed. Fig. 2 also reveals that while the length of C-N breaking bond in **TS3** is 1.90 Å, the C-H breaking and H-N forming bonds in **TS4** are 1.24 and 1.61 Å, respectively. A deep attention to Fig. 2 implies that neither forming-breaking bond lengths nor corresponding imaginary frequencies are markedly affected in the presence of solvent. The latter is a

direct consequence of this fact that barrier heights remain roughly unchanged in going from gas to the solvent phase.

(ii) DFT analysis based on the global and local reactivity indexes.

Studies devoted to cycloaddition reactions [28-33] have shown that the global indices defined within the conceptual DFT [34,35] are powerful tool to explain the reactivity and regioselectivity in the 32CA reactions. The global indexes, namely, electronic chemical potential (μ), chemical hardness (η), global electrophilicity (ω), and global nucleophilicity (*N*) for nitrile imine **6** and enamine **7** are presented in Table 2. The electronic chemical potential of enamine **7**, -2.92 eV, is higher than that of nitrile imine **6**, -4.52 eV, indicating that nitrile imine **6** and enamine **7** will act as electrophile and nucleophile, respectively, along a polar cycloaddition reaction. Consequently, along the corresponding 32CA reaction the global electron density transfer (GEDT) will take place from the enamine **7** towards the nitrile imine **6**, in clear agreement with the GEDT analysis performed on the corresponding TSs; the GEDT from enamine **7** to the nitrile imine **6** is 0.20 ē at **TS1** and 0.19 ē at **TS2**. These very similar GEDTs indicate that the 32CA reaction under investigation presents some polar character in both regioisomeric pathways. The global electrophilicity index for nitrile imine **6**, 2.38 eV, and enamine **7**, 0.84 eV, allows these compounds to be classified as strong and moderate electrophiles, respectively, within the electrophilicity scale [36]. On the other hand, the global nucleophilicity index for nitrile imine **6**, 2.45 eV, and enamine **7**, 3.67 eV, permits them to be categorised as moderate and strong nucleophiles, respectively [37]. Analysis of these global indices indicates that along a polar 32 CA reaction, nitrile imine **6** will act as strong electrophile while enamine **7** will act as strong nucleophile. When an electrophile-nucleophile pair is approached, the most favorable reactive channel is that associated with the initial two-center interaction between the most electrophilic center of electrophile and the most nucleophilic center of nucleophile. Recently, Domingo have proposed the electrophilic P_k^+ and nucleophilic P_k^- Parr functions derived from the excess of spin electron density reached *via* the GEDT process from the nucleophile to the electrophile as powerful tool in the study of the local reactivity in polar processes [23]. Herein, in order to explain regioselectivity observed experimentally in the reaction under

study, Parr functions including corresponding local reactivity indexes for reactive sites directly involved in the 32CA reaction between nitrile imine **6** and enamine **7** are analysed. As nitrile imine **6** and enamine **7**, respectively, act as electrophile and nucleophile; the electrophilic Parr function, P_k^+, for N1 and C3 atoms of nitrile imine **6** and nucleophilic Parr function, P_k^-, for C4 and C5 atoms of enamine **7** (see Scheme 4 for atoms numbering) are calculated and depicted in Fig. 3. As mentioned in the computational section, calculating local reactivity indexes will be so simple with the Parr functions at hand. Considering Parr functions presented in Fig. 3, the local electrophilicity index, ω_k, for N1 and C3 atoms of nitrile imine **6** is -0.07 and 0.62 eV, respectively. On the other hand, the local nucleophilicity index, N_k, for C4 and C5 atoms of enamine **7** is -0.44 and 2.01 eV, respectively. It should be noted that negative values of ω_k for N1 atom of nitrile imine **6** and N_k for C4 atom of enamine **7** are a direct consequence of the negativity found for their corresponding Parr functions indicating local deactivation of these centers [22]. The most electrophilic activation found on C3 atom of nitrile imine **6** and the most nucleophilic activation found on C5 atom of enamine **7**, in one hand, and deactivations found on the N1 and C4 atoms of these reactants, in other hand, is responsible for the two-center C3-C5 interaction found at **TS1** leading to the more favorable N1-C4 regioisomeric pathway along corresponding 32CA reaction. In the other words, the regioselectivity predicted according to the calculated local reactivity indexes is in excellent agreement with the unique regioisomeric celecoxib **3** observed experimentally.

4. Conclusion

Based on the molecular mechanism and energetic studies performed in this work using DFT methods at the B3LYP/6-31G* level, considering the protocol introduced by Oh, the synthesis of celecoxib **3** takes place via a domino process initialised by a 32CA reaction between nitrile imine **6** and enamine **7** followed by an acid/base catalysed stepwise morpholine elimination yielding celecoxibe **3**. Due to the asymmetric nature of nitrile imine **6** and enamine **7**, two competitive N1-C4 and N1-C5 regioisomeric pathways can be found in the 32CA reaction. The calculated activation Gibbs free energies clearly

show that **TS1** associated with the N1-C4 regioisomeric pathway is significantly favored over **TS2** corresponded to the N1-C5 one, ruling out the later regioisomeric channel. Consequently, the 32CA reaction of this domino process, which corresponds to the rate-determining step of the overall domino process, is completely regioselective yielding, via **TS1**, CA **8**. The subsequent protonation of CA **8** yields intermediate **11** which in turn experiences a morpholine elimination reaction via a very low energetic **TS3** affording cationic intermediate **12** that is converted into the celecoxibe **3** through a barrierless proton abstraction step. In summary, as Oh described, the synthesis of celecoxib **3** is so simple, straightforward, and also rapid. Analysis of the local reactivity indexes using calculated electrophilic and nucleophilic Parr functions at the reactive sites of starting material clearly reveals why the 32CA reaction under investigation presents a complete regioselective fashion in excellent agreement with the experiment.

Supporting information

B3LYP/6-31G* total electronic energies including thermochemical data together with the Cartesian coordinates of the optimised structures in the gas phase, involved in the studied domino reaction are given in the supporting information.

Acknowledgment

The author presents special thanks to Professor Luis. R. Domingo in Universidad de Valencia of Spain for so helpful and effective comments leading to considerably improvement of the initial draft.

References

[1] R. M. Rao, G. N. Reddy, J. Sreeramulu, Synthesis of some new pyrazolo-pyrazole derivatives containing indoles with antimicrobial activity, Der. Pharma. Chem. 3 (2011) 301-309.

[2] S. Ningaiah, S. D. Doddaramappa, Chandra, M. Madegowda, S. Keshavamurthy, U. K. Bhadraiah, One-Pot Tandem Synthesis of Tetrasubstituted Pyrazoles via 1,3-Dipolar Cycloaddition Between Aryl Hydrazones and Ethyl But-2-ynoate, Synthetic Commun. 44 (2014) 2222-2231.

[3] E. M. Sharshira, N. M. M. Hamada, Synthesis and Antimicrobial Evaluation of Some Pyrazole Derivatives, Molecules 17(2012) 4962-4971.

[4] P. Khloya, P. Kumar, A. Mittal, N. K. Aggarwal, P. K. Sharma, Synthesis of some novel 4-arylidene pyrazoles as potential antimicrobial agents, Org. Med. Chem. Lett. 3 (2013) 9-16.

[5] J. Z. Chandanshive, P. B. Gonzalez, W. Tiznado, B. F. Bonini, J. Caballero, C. Femoni, M. C. Franchini, 1,3-Dipolar cycloaddition of nitrile imines with α,β-unsaturated lactones, thiolactones and lactams: synthesis of ring-fused pyrazoles, Tetrahedron 68 (2012) 3319-3328.

[6] A. K. Tewari, V. P. Singh, P. Yadav, G. Gupta, A. Singh, R. K. Goel, P. Shinde, C. G. Mohan, Synthesis, biological evaluation and molecular modeling study of pyrazole derivatives as selective COX-2 inhibitors and anti-inflammatory agents, Bioorg. Chem. 56 (2014) 8-15.

[7] L. M. Oh, Synthesis of celecoxib via 1,3-dipolar cycloaddition, Tetrahedron Lett. 47 (2006) 7943-7946.

[8] L. R. Domingo, J. A. Sáez, J. A. Joule, L. Rhyman, P. Ramasami, A DFT Study of the [3 + 2] versus [4 + 2] Cycloaddition Reactions of 1,5,6-Trimethylpyrazinium-3-olate with Methyl Methacrylate, J. Org. Chem. 78 (2013) 1621−1629.

[9] D. H. Ess, K. N. Houk, Theory of 1,3-Dipolar Cycloadditions: Distortion/Interaction and Frontier Molecular Orbital Models, J. Am. Chem. Soc. 130 (2008) 10187–10198.

[10] C. Lee, W. Yang, R. G. Parr, Development of the Colle-Salvetti correlation-energy formula into a functional of the electron density, Phys. Rev. B. 37 (1988) 785-789.

[11] X. Li, M. J. Frisch, Energy-Represented Direct Inversion in the Iterative Subspace within a Hybrid Geometry Optimization Method, J. Chem. Theory and Comput. 2 (2006), 835-839.

[12] K. Fukui, Formulation of the reaction coordinate, J. Phys. Chem. 74 (1970), 4161-4163.

[13] H. P. Hratchian, H. B. Schlegel, Accurate reaction paths using a Hessian based predictor-corrector integrator, J. Chem. Phys. 120 (2004) 9918-9924.

[14] H. P. Hratchian, H. B. Schlegel, Using Hessian updating to increase the efficiency of a Hessian based predictor-corrector reaction path following method, J. Chem. Theory and Comput. 1 (2005) 61-69.

[15] J. Tomasi, M. Persico, Molecular Interactions in Solution: An Overview of Methods Based on Continuous Distributions of the Solvent, Chem. Rev. 94 (1994) 2027-2094.

[16] E. Cances, B. Mennucci, J. Tomasi, A new integral equation formalism for the polarizable continuum model: Theoretical background and applications to isotropic and anisotropic dielectrics, J. Chem. Phys. 107 (1997) 3032-3041.

[17] M.Cossi, V.Barone, R.Cammi, J. Tomasi, Ab initio study of solvated molecules: a new implementation of the polarizable continuum model, Chem. Phys. Lett. 255 (1996) 327-335.

[18] V. Barone, M. Cossi, J. Tomasi, Geometry optimization of molecular structures in solution by the polarizable continuum model, J. Comput. Chem. 19 (1998) 404-417.

[19] A. E. Reed, F. Weinhold, Natural bond orbital analysis of near-Hartree–Fock water dimer, J. Chem. Phys. 78 (1983) 4066-4073.

[20] R. G. Parr, L. Von Szentpaly, S. Liu, Electrophilicity Index, J. Am. Chem. Soc. 121 (1999) 1922-1924.

[21] T. A. Koopmans, Über die Zuordnung von Wellenfunktionen und Eigenwerten zu den einzelnen Elektronen eines Atoms, Physica1, 1-6 (1934), 104-113.

[22] L. R. Domingo, P. Perez, D. E. Ortega, Why Do Five-Membered Heterocyclic Compounds Sometimes Not Participate in Polar Diels–Alder Reactions?, J. Org. Chem. 78 (2013) 2462-2471.

[23] L. R. Domingo, P. Perez, J. A. Saez, Understanding the local reactivity in polar organic reactions through electrophilic and nucleophilic Parr functions, RSC Adv. 3 (2013) 1486-1494.

[24] M. J. Frisch, G. W. Trucks, H. B. Schlegel, G. E. Scuseria, M. A. Robb, J. R. Cheeseman, G. Scalmani, V. Barone, B. Mennucci, G. A. Petersson, H. Nakatsuji, M. Caricato, X. Li, H. P. Hratchian, A. F. Izmaylov, J. Bloino, G. Zheng, J. L. Sonnenberg, M. Hada, M. Ehara, K. Toyota, R. Fukuda, J. Hasegawa, M. Ishida, T. Nakajima, Y. Honda, O. Kitao, H. Nakai, T. Vreven, J. A. Montgomery, Jr., J. E. Peralta, F. Ogliaro, M. Bearpark, J. J. Heyd, E. Brothers, K. N. Kudin, V. N. Staroverov, R. Kobayashi, J. Normand, K. Raghavachari, A. Rendell, J. C. Burant, S. S. Iyengar, J. Tomasi, M. Cossi, N. Rega, J. M. Millam, M. Klene, J. E. Knox, J. B. Cross, V. Bakken, C. Adamo, J. Jaramillo, R. Gomperts, R. E. Stratmann, O. Yazyev, A. J. Austin, R. Cammi, C. Pomelli, J. W. Ochterski, R. L. Martin, K. Morokuma, V. G. Zakrzewski, G. A. Voth, P. Salvador, J. J. Dannenberg, S. Dapprich, A. D. Daniels, O. Farkas, J. B. Foresman, J. V. Ortiz, J. Cioslowski, D. J. Fox, Gaussian 09 (Revision A.02-SMP) (Gaussian Inc., Wallingford, CT, 2009).

[25] K.W. Wiberg, Application of the pople-santry-segal CNDO method to the cyclopropylcarbinyl and cyclobutyl cation and to bicyclobutane, Tetrahedron 24 (1968) 1083-1096.

[26] M. C. Aversa, A. Barattucci, P. Bonaccorsi, A. Contini, Addition of sulfenic acids to monosubstituted acetylenes: a theoretical and experimental study, J. Phys. Org. Chem., 22 (2009), 1048–1057.

[27] L. R. Domingo, J. A. Saéz, R. J. Zaragozá M. Arnó, Understanding the Participation of Quadricyclane as Nucleophile in Polar [2σ + 2σ + 2π] Cycloadditions toward Electrophilic π Molecules, J. Org. Chem. 73 (2008) 8791-8799.

[28] L. R. Domingo, A density functional theory study for the Diels–Alder reaction between *N*-acyl-1-aza-1,3-butadienes and vinylamines. Lewis acid catalyst and solvent effects, Tetrahedron 58 (2002), 3765-3774.

[29] L. R. Domingo, M. J. Aurell, Density Functional Theory Study of the Cycloaddition Reaction of Furan Derivatives with Masked *o*-Benzoquinones. Does the Furan Act as a Dienophile in the Cycloaddition Reaction?, J. Org. Chem. 67 (2002) 959-965.

[30] L. R. Domingo, M. J. Aurell, P. Pérez, and R. Contreras, Origin of the Synchronicity on the Transition Structures of Polar Diels−Alder Reactions. Are These Reactions [4 + 2] Processes?, J. Org. Chem. 68 (2003) 3884-3890.

[31] L. R. Domingo, J. Andrés, Enhancing Reactivity of Carbonyl Compounds via Hydrogen-Bond Formation. A DFT Study of the Hetero-Diels−Alder Reaction between Butadiene Derivative and Acetone in Chloroform, J. Org. Chem. 68 (2003) 8662-8668.

[32] L. R. Domingo, Why do Electron-Deficient Dienes React Rapidly in Diels−Alder Reactions with Electron-Deficient Ethylenes? A Density Functional Theory Analysis, Eur. J. Org. Chem. 2004 (2004), 4788-4793.

[33] P. Arroyo, M. T. Picher, L. R. Domingo, F. Terrier, A DFT study of the polar Diels–Alder reaction between 4-aza-6-nitrobenzofuroxan and cyclopentadiene, Tetrahedron 61 (2005) 7359-7365.

[34] P. Geerlings, F. De Proft, W. Langenaeker, Conceptual Density Functional Theory, Chem. Rev. 103 (2003), 1793-1874.

[35] D. Ess, G. O. Jones, K. N. Houk, Conceptual, Qualitative, and Quantitative Theories of 1,3-Dipolar and Diels–Alder Cycloadditions Used in Synthesis, Adv. Synth. Catal. 348 (2006) 2337-2361.

[36] L. R. Domingo, M. j. Aurell, P. Perez, R. Contreras, Quantitative characterization of the global electrophilicity power of common diene/dienophile pairs in Diels–Alder reactions, Tetrahedron 58 (2002) 4417-4423.

[37] P. Jarmillo, L. R. Domingo, E. Chamorro, P. Perez, A further exploration of a nucleophilicity index based on the gas-phase ionization potentials, J. Mol. Struct. (THEOCHEM) 865 (2008) 68-72.

Caption of figures:

Figure 1. Relative Gibbs free energy profile, in the presence of THF, for the proposed mechanism presented in scheme 4 associated with the domino reaction between nitrile imine **6** and enamine **7** yielding celecoxibe **3**.

Figure 2. B3LYP/6-31G* optimised geometries including corresponding imaginary frequencies (in cm^{-1}) for TSs involved in the 32CA reaction step, **TS1** and **TS2**, and those involved in the morpholine elimination step, **TS3** and **TS4** of the studied domino reaction in the gas phase. Selected bond distances are given in Å. Corresponding values in the presence of THF are given in the parentheses. Hydrogens of enamine moiety were omitted for clarity.

Figure 3. B3LYP/6-31G* maps of ASD (Atomic Spin Densities) including electrophilic Parr functions, P_k^+, for N1 and C3 atoms of the radical anion of nitrile imine **6** and maps of ASD including nucleophilic Parr functions, P_k^-, for C4 and C5 atoms of the radical cation of enamine **7**. Atoms numbering is displayed in Scheme 4.

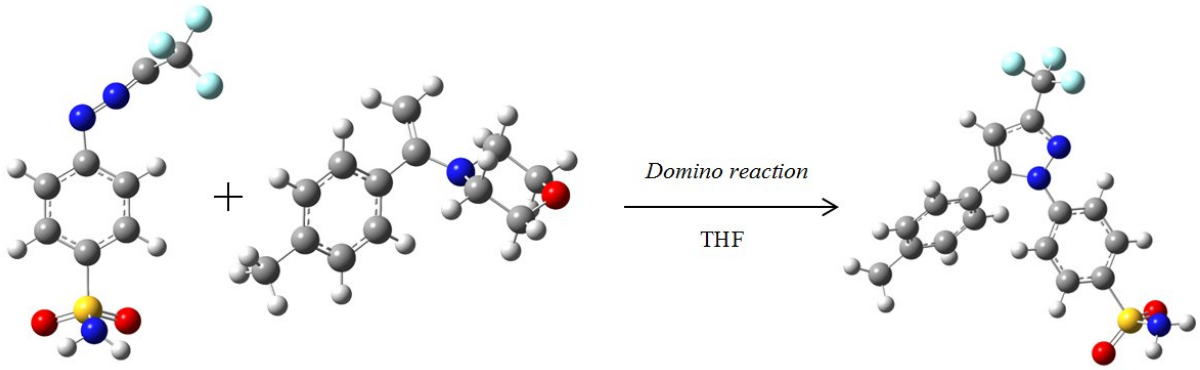

Nitrile imine Enamine Celecoxib

- The celecoxib synthesis via a domino reaction was theoretically studied using DFT.
- [3+2] cyclisation step presents a complete regioselective fashion.
- Mechanism and activation barriers are not considerably affected by solvent.
- The experimental outcomes can nicely be explained using DFT reactivity indices.

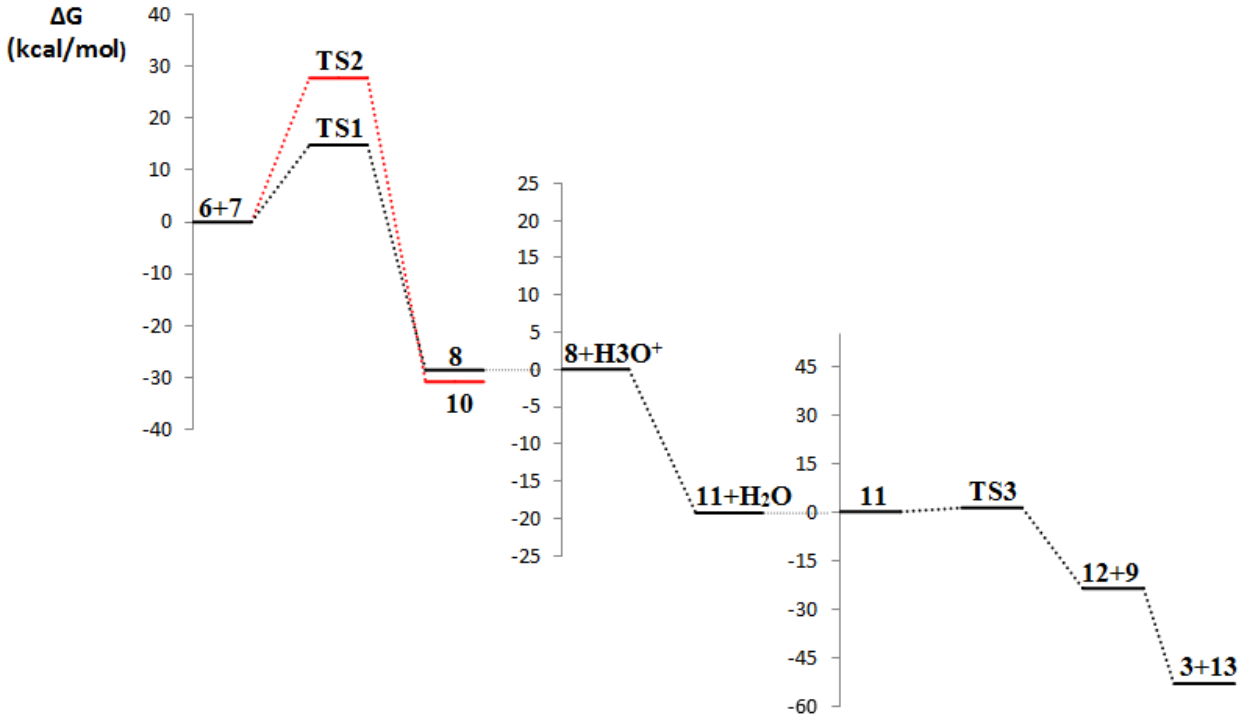

Fig. 1.

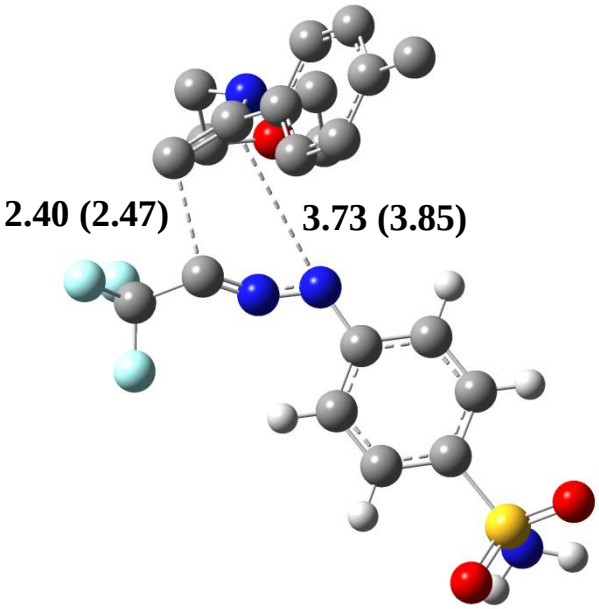

TS1

-133.5 (-139.4) cm^{-1}

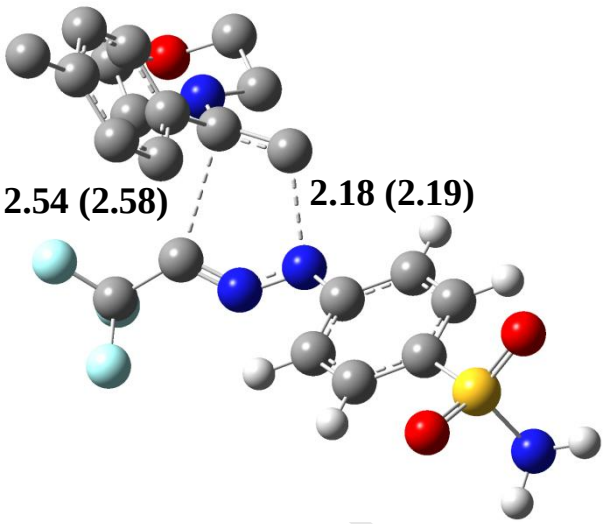

TS2

-294.2 (-296.7) cm^{-1}

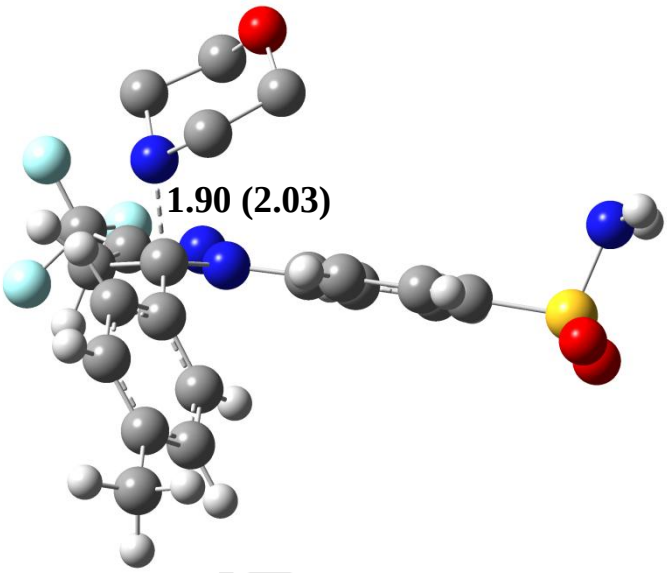

TS3

-165.2 (-164.5) cm^{-1}

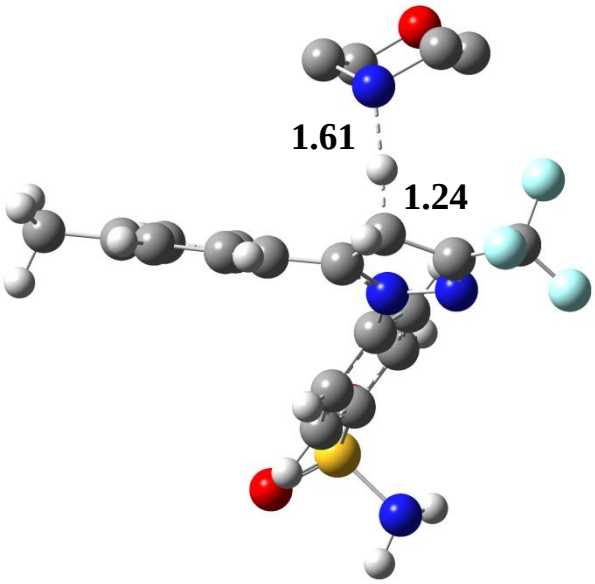

TS4

-212.1cm^{-1}

Fig. 2.

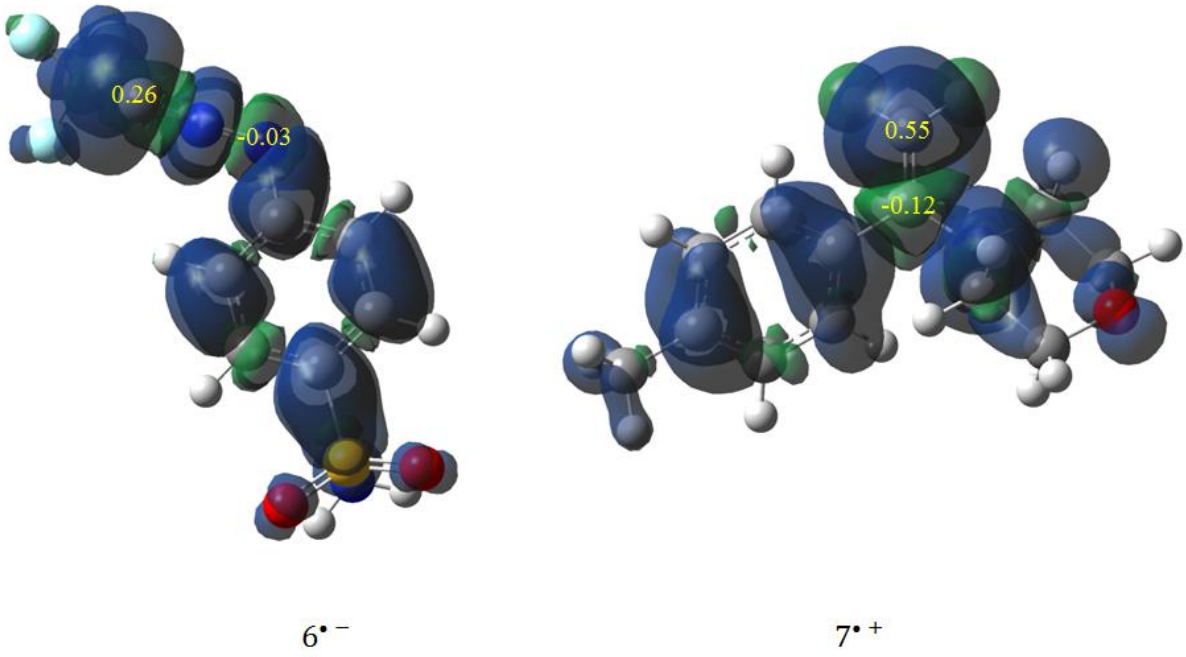

Fig. 3.

Table 1. B3LYP/6-31G* Gibbs free energies (G) and its relative (ΔG) values for various species involved in the studied domino reaction

	Gas phase (ε = 1.00)		THF (ε = 7.42)	
Species	G (a.u.)	ΔG (kcal/mol)	G (a.u.)	ΔG (kcal/mol)
6	-1320.609054		-1320.619785	
7	-635.330185		-635.334777	
TS1	-1955.914844	15.3[a]	-1955.930984	14.8[a]
8	-1955.981276	-26.4[a]	-1956.000050	-28.5[a]
TS2	-1955.894321	28.2[a]	-1955.910348	27.7[a]
10	-1955.986932	-29.9[a]	-1956.003587	-30.8[a]
H_3O^+	-76.672899		-76.781137	
8+ H_3O^+	-2032.654175		-2032.781187	
11	-1956.330516		-1956.400402	
H_2O	-76.405452		-76.411492	
11+ H_2O	-2032.735968	-51.3[b]	-2032.811894	-19.3[b]
TS3	-1956.329874	0.4[c]	-1956.398489	1.2[c]
12	-1668.682293		-1668.748033	
9	-287.685842		-287.690153	
12+9	-1956.368135	-23.6[c]	-1956.438186	-23.7[c]
TS4	-1956.367741	-23.4[c]	N/A*	
3	-1668.351455		-1668.362691	
13	-288.041567		-288.122408	
3+13	-1956.393022	-39.2[c]	-1956.485099	-53.1[c]

a: Relative to (6+7).

b: Relative to (8+H_3O^+).

c: Relative to 11.

*: Not available (any attempt to locate TS4 failed in the presence of THF).

Table 2. B3LYP/6-31G* electronic chemical potential, μ, chemical hardness, η, global electrophilicity, ω, and global nucleophilicity, *N*, in eV, for nitrile imine **6** and enamine **7**

Species	μ	η	ω	*N*
Nitrile imine **6**	-4.52	4.29	2.38	2.45
Eneamine **7**	-2.92	5.05	0.84	3.67